Revised version (clean copy)

Supplementary Data

Tables

Table S1. Key Resources

REAGENT or RESOURCE	SOURCE	IDENTIFIER
Antibodies		
mouse Anti-human IgG1	ZSGB-BIO	Ca#ZM-0491
Rabbit Anti-human IgG2	Abcam	Ca#134050
Rabbit Anti-human IgG3	Abcam	Ca#109761
Rabbit Anti-human IgG4	Abcam	Ca#109493
Rabbit Anti-CD8 monoclonal antibody	ZSGB-BIO	Cat#ZA-0508
mouse Anti-human cytokeratin	ZSGB-BIO	Ca#ZM-0069
Rituximab	F.Hoffmann-la Roche Limited	
Cetuximab	Rilisheng	
Nivolumab	Bristol-Myers Squibb Holdings Pharma, Ltd.Liability Company	
Goat Anti-Rabbit IgG 680	LI-COR	Cat#9266680070
Goat Anti-Mouse IgG(H+L) Alexa Fluor 488	Thermo Scientific	Cat#A31619
Goat Anti-Mouse IgG(H+L) Alexa Fluor 555	Thermo Scientific	Cat#A31621
Goat Anti-Rabbit IgG(H+L) Alexa Fluor 488	Thermo Scientific	Cat#A31627
Goat Anti-Rabbit IgG(H+L) Alexa Fluor 555	Thermo Scientific	Cat#A31629
Two-step IHC test kit	ZSGB-BIO	Cat#PV-9000
Mouse Anti-Insulin	ZSGB-BIO	Cat#ZM-0155
Mouse Anti-PCNA	ZSGB-BIO	Cat#ZM-0213
Mouse Anti-Neurofilament	ZSGB-BIO	Cat#ZM-0198
Mouse Anti-Glucagon	ZSGB-BIO	Cat#ZA-0119
Biological Samples		
Healthy adult blood	Shantou university Affiliated second Hospital	N/A
ESCA adult blood	Shantou university Affiliated Tumor Hospital	N/A
ESCA adult Esophageal tissue	Shantou university Affiliated Tumor Hospital and the East Guangdong Provincial Pathological Consultation Center	N/A
Chemicals, Peptides, and Recombinant Proteins		

Recombinant Protein G Agarose	Invitrogen by Life technologies	Cat#15920010
IgG1	Athens research & Technology GA.USA	Cat#16160907071 M
IgG2	Athens research & Technology GA.USA	Cat#16160907072 M
IgG3	Athens research & Technology GA.USA	Cat#16160907073
IgG4	Athens research & Technology GA.USA	Cat#16160907074 M
AEC kit	golden bridge international	Cat#ZLI-9036
IgG4 ELISA kit	Neobioscience Technology，Shenzhen, China	Cat#EHC147.96
Natural human IgG1 protein	Abcam	Cat#ab90283
Natural human IgG2 protein	Abcam	Cat#ab90284
Natural human IgG3 protein	Abcam	Cat#ab118426
Natural human IgG4 protein	Abcam	Cat#ab90286
IgA	Abcam	Cat#ab91025
IgE	Abcam	Cat#ab90392
IgM	Abcam	Cat#ab91117
IgD	Abcam	Cat#ab91002
12-O-tetradacanoylphorbol-13-acetate (TPA)	Sigma	Cat#P1585
7,12-dimethylbenz (a) anthracene (DMBA)	Sigma	Cat#D3245
IVIG	Rongsheng	Cat#603J
Critical Commercial Assays		
Roche immune turbidimetry method	Golden Field Medical Test Company	
Pierce™ BCA Protein Assay Kit	Thermo Scientific	Cat#23225
Pierce™ Fab Preparation Kit	Thermo Scientific	Cat#44985
AnaTag™ Biotin Protein Labeling Kit	Ana spec	Cat#AS-72057
Human IgG1 affinity matrix	Thermo Scientific	Cat#191303010
Human IgG4 affinity matrix	Thermo Scientific	Cat#290005
Experimental Models: Cell Lines		
A549	Cell bank of Chinese Academy of Sciences	Cat #SCSP-503
U937	Procell Life Science & Technology	Cat #CL-0239
Raji	Cell bank of Chinese Academy of Sciences	Cat #TCHu 44
4T1	Cell bank of Chinese Academy of Sciences	Cat #TCM32

CT26.WT	Cell bank of Chinese Academy of Sciences	Cat #TCM37
Experimental Models: Organisms/Strains		
Immune potent BALB/C mice	Vital River technical co.	
Software and Algorithms		
GraphPad Prism 7	GraphPad Software	https://www.graphpad.com/scientific-software/prism/
Image J	N/A	https://imagej.nih.gov/ij/index.html

Table S2. Human Tissue and Blood Sample

All tissue and blood samples were obtained with patients' consent, and approved by The Ethics Committee of Shantou University Medical College. Pathological diagnostic criteria were based on the eighth edition of the AJCC guidelines.

Tissue samples		
Esophageal cancer tissue	1100~~02~~ Cases	Source: Shantou university Affiliated Tumor Hospital
Adjacent esophageal cancer tissue	6~~1~~0 Cases	Source: Shantou university Affiliated Tumor Hospital
Normal esophageal mucous tissue	63~~53~~ Cases	Source: Shantou university Affiliated Tumor Hospital
Total	233~~165~~ Cases	
Blood samples		
Esophageal cancer patients' blood sample	82 Cases	Source: Shantou university Affiliated Tumor Hospital
Healthy volunteers' blood sample	70 Cases	Source: Shantou university Affiliated second Hospital
Total	152 Cases	

Figures and legends

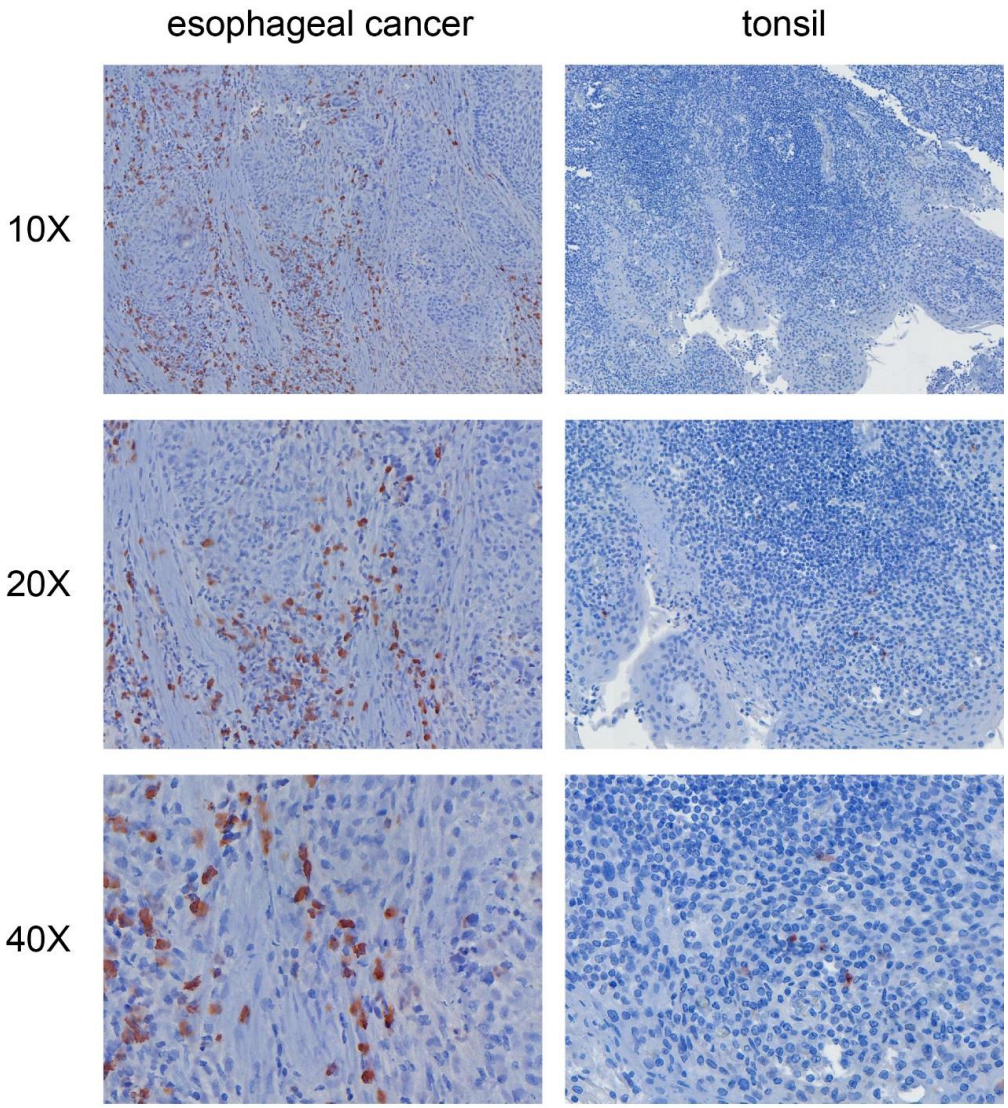

Figure S1. Increase of IgG4-containing B lymphocytes in cancer.

Esophageal cancer tissue sample and normal tonsil tissue sample immunostained with monoclonal antibody to IgG4 at different magnifications. It clearly showed that IgG-positive lymphocytes were marked increased in number in cancer tissue (left column) in comparison to normal lymphoid tissue (right column). In normal mucosa and lymphoid tissues IgG4-positive lymphocytes were barely detectable.

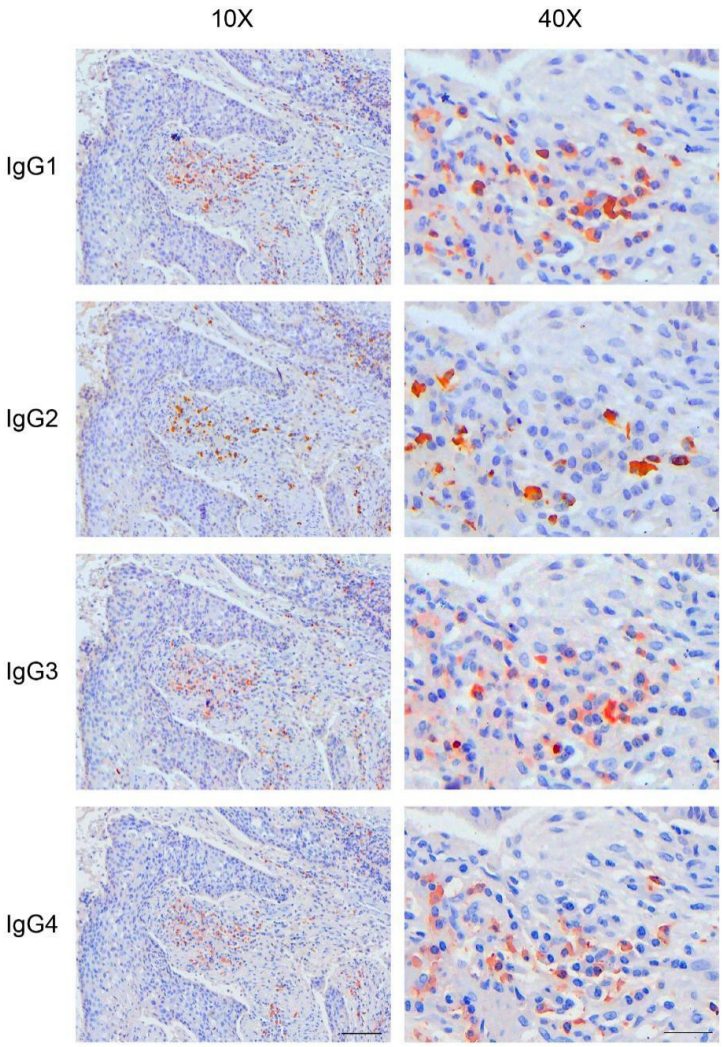

Figure S2. Abundance and distribution of IgG subtypes in cancer microenvironment

Figure S2A. Intermediate steps of the SDS methods, in which IgG1, 2, 3 and 4 were immunostained sequentially on the same esophageal cancer tissue section. The color labeling was photographed after each antigen staining and then the bound antibodies together with the labeling were eluted. The four separate staining results were integrated into a simple photo with an image editing software (Photoshop) as shown in Figure 1H&1I. It shows that IgG4 positive cells were markedly increased.

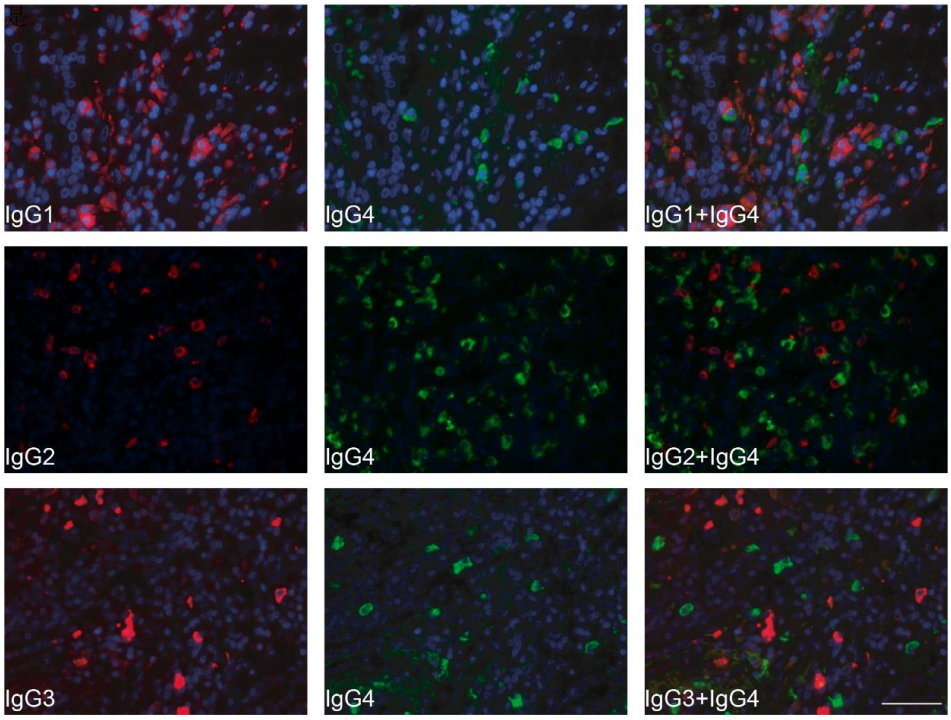

Figure S2B. Double immunostaining of IgG1, 2 or 3 (red fluorescence) and IgG4 (green fluorescence) on the same cancer tissue section viewed with a confocal fluorescence microscope. The results show that IgG4-positive lymphocytes (green fluorescence) were often in close proximity or partially overlapping to IgG1-positive or IgG2-positive cells but not to IgG3-positive cells.

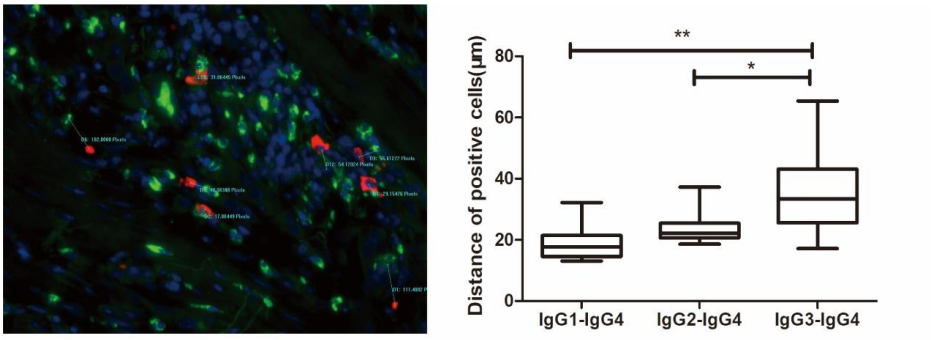

*Figure S2C. The physical distances between different B lymphocytes (labeled by red and green fluorescence separately) were measured and analyzed with an Image Pro Plus software on 10 cases of esophageal cancers (5 high power fields each) (left). The cell distance between IgG4 and IgG3 positive cells was larger than that between IgG4 and IgG1 (**p<0.01), or that between IgG4 and IgG2 (*p<0.05) (right). The significance of this observation will be addressed in a*

separate report.

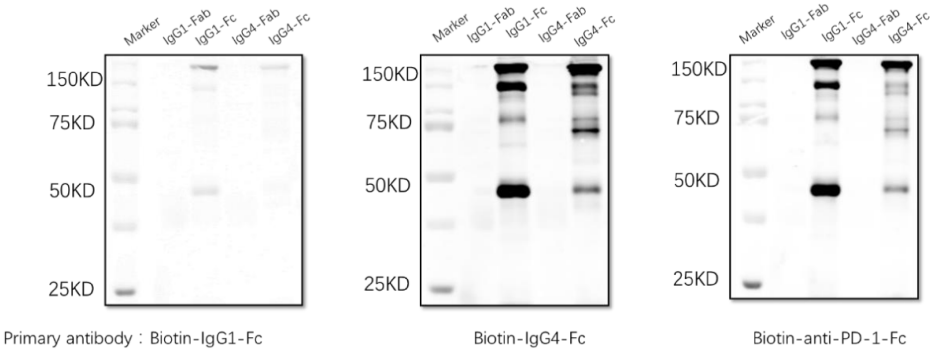

Figure S3. Western blot of non-reducing gel showing Fc-Fc reaction between IgG4 and IgG1(also weakly between IgG4 and IgG4)

Results showed that IgG4 Fc fragment reacted to IgG1 Fc but not to IgG1 Fab (middle). We also tested antibody to PD-1 (Nivolumab, IgG4 subtype) that also showed Fc-Fc reaction to IgG1 (right). IgG1 Fc did not react to IgG1 or IgG4 (Fc or Fab) (left).

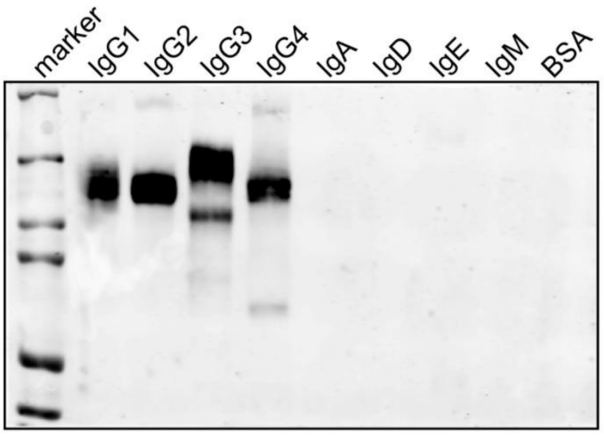

Figure S4. Western blot electrophoresis of human reacting to immunoglobulin subclasses.

The results showed that human IgG4 reacted to human IgG1, 2, 3 and 4, but not to human IgA, IgD, IgE, IgM and the negative control BSA.

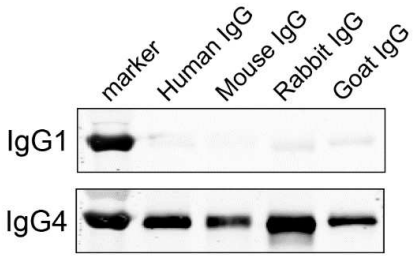

Figure S5. Western blot of human IgG4 reactions to IgG of different species.

The results showed that human IgG4, but not human IgG1, reacted to IgGs from human, mouse, rabbit and goat.

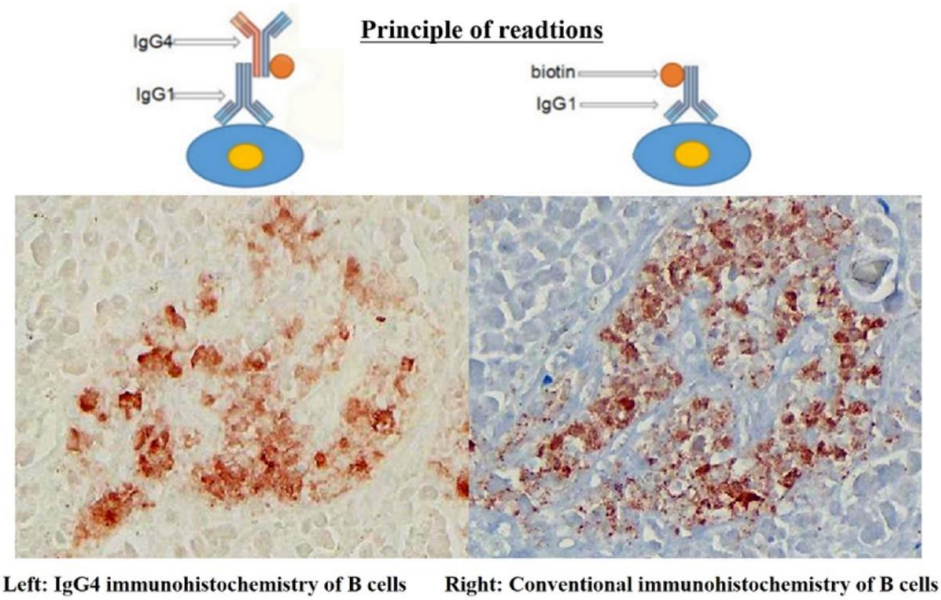

Figure S6. The Fc-Fc reaction between IgG4 and IgG1 bound to tissue sections was further tested and validated with a number of antibodies and tissue types apart from cancer

We tested the ability of IgG4 to react to tissue-bound IgG1 with a number of IgG1 antibodies on different tissue types. Left photo shows an example of biotin-labeled IgG4 reacting to antibody (IgG1) to insulin in beta cells of human pancreas. In this case, the primary antibody against insulin was first applied to pancreatic tissue section followed by applying biotin-labeled IgG4 (not specifically against IgG4 or insulin). The labeling biotin was then visualized with a AEC detecting kit (left). With this method, insulin-containing beta cells was clearly demonstrated that is comparable to that visualized with conventional immunohistochemistry (right). This demonstrates that IgG4 could bind to IgG1 via Fc-Fc reaction that has been immobilized to tissue antigens.

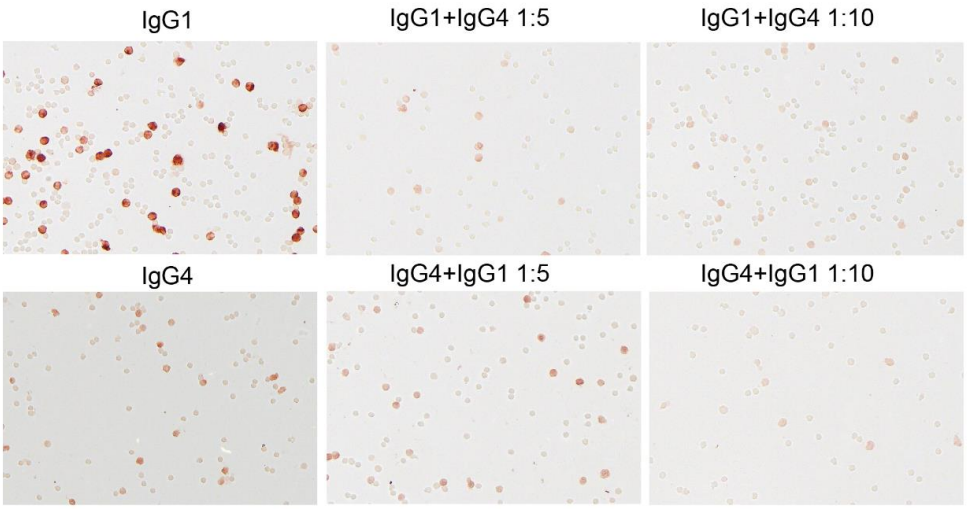

Figure S7. IgG4 and IgG1 competed with one another in binding to Fc receptors of monocytes. *IgG1 and IgG4 were both found to react to peripheral blood monocytes and they competed in binding to monocyte Fc receptors, i.e. when the concentration of unlabeled IgG4 was increased, labeled IgG1 positive cells were decreased, although it can be seen that the binding of IgG4 to PBMC was weaker than that of IgG1. The reverse is also true, i.e. when the concentration of unlabeled IgG1 was increased, labeled IgG4 positive cells were decreased.*

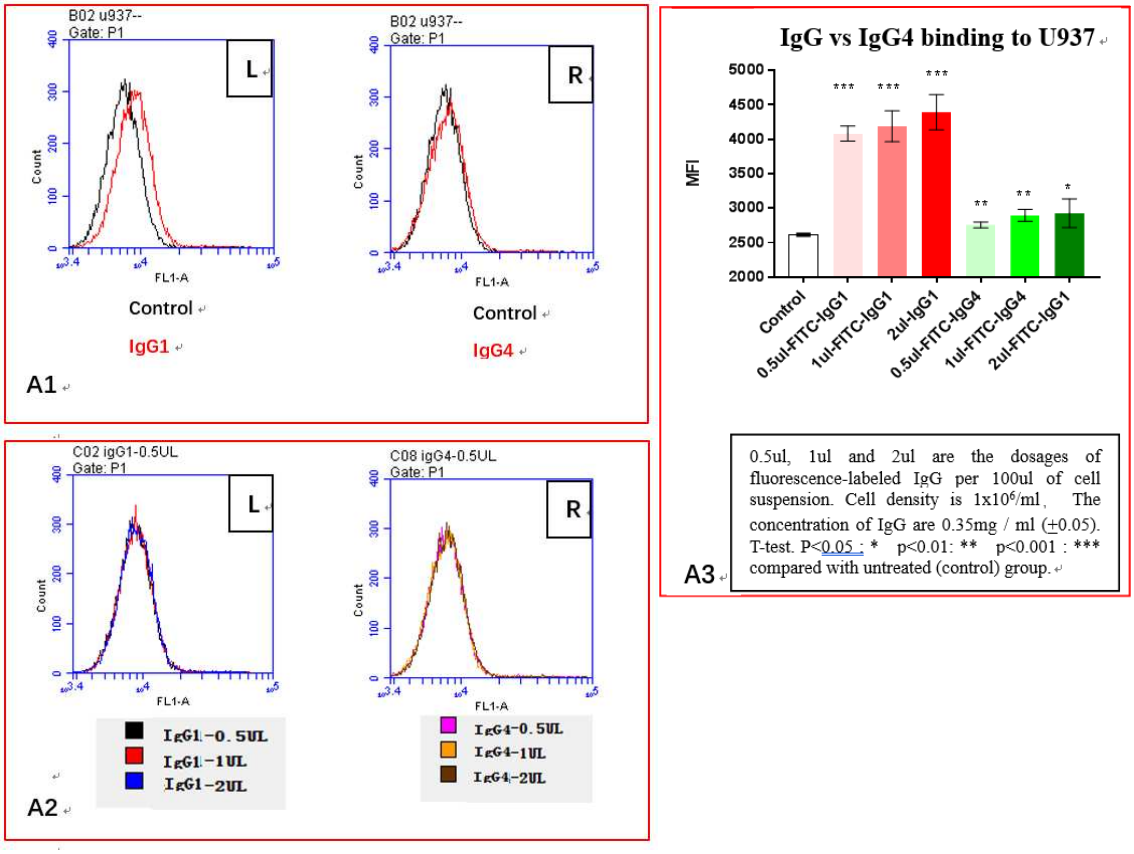

Figure S8. Competition between IgG1 and IgG4 to bind to Fc receptors (FITC-labeled assays)

A: Flowcytometry showing both IgG1 & IgG4 can bind to monocytes

FITC-labeled IgG incubated with U937 cells at 4℃ for 15mins, washed away excess fluorescent protein, used BD C6 flow cytometer to measure cell fluorescence intensity. Negative controls were cells not treated with fluorescent protein.

***A1:** FITC labeled IgG1 (left) and IgG4 (right) bind to U937, the horizontal coordinate represents fluorescence intensity (FI), the vertical coordinate represents number of cells in this FI. The FI of IgG1 group is higher than that in IgG4 group, indicating that IgG1 has a stronger binding force than IgG4. **A2:** With the increase of IgG1(L) and IgG4(R) concentrations, the cell FI did not have significant changes ($p>0.05$, 0.5μL, 1μL and 2μL are the dosages of fluorescence-labeled IgG per 100μL cell suspension) indicating that the binding of IgG and cells reached saturation. **A3:** This is a summary of A1 and A2. Mean fluorescence intensity (MFI) represents the average binding force of IgG on U937 (1×10^4 cells), the binding force of IgG1 on U937 cells was higher than that of IgG4 on U937 cells. ($p<0.001$).*

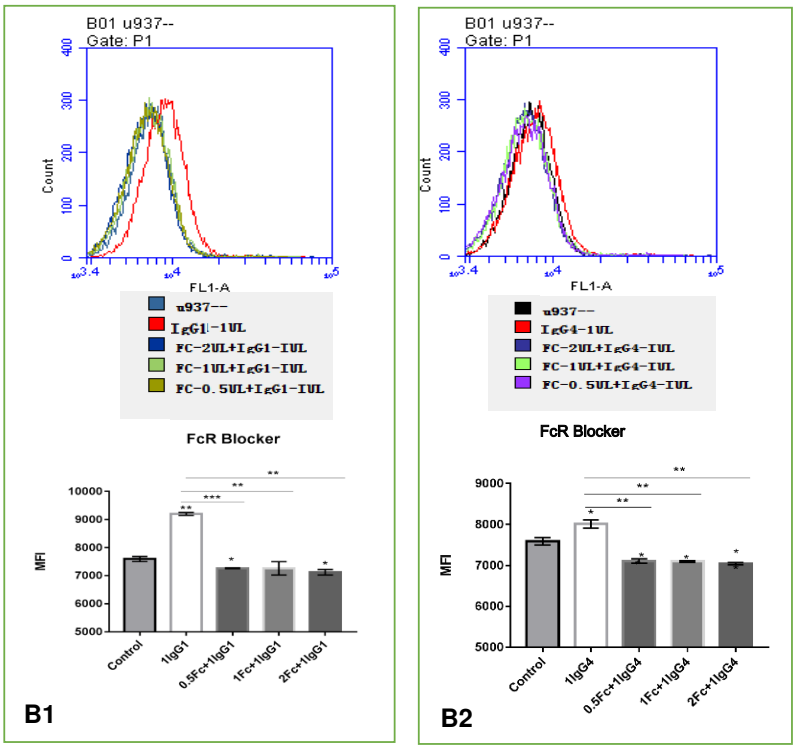

B: The bindings could be blocked by Fc blocker

To verify IgG binding sites on U937, we used Fc receptor blockers to block all Fc receptors on U937, and then used FITC-labeled IgG to incubate with FcR blocked U937 at 4°C for 15mins, washed away excess fluorescent protein, and then used BD C6 flow cytometer to measure cell fluorescence intensity. Unblocked U937 was used as the positive control.

***B1:** The binding between IgG1 and U937 cells was blocked by Fc receptor blocker. Compared with the positive group (white). ($p<0.001$) The blocking effects of 0.5 unit, 1 unit and 2 unit dosages of receptor blocker were consistent. ($p>0.05$). **B2:** The results of IgG4 were consistent with IgG1.*

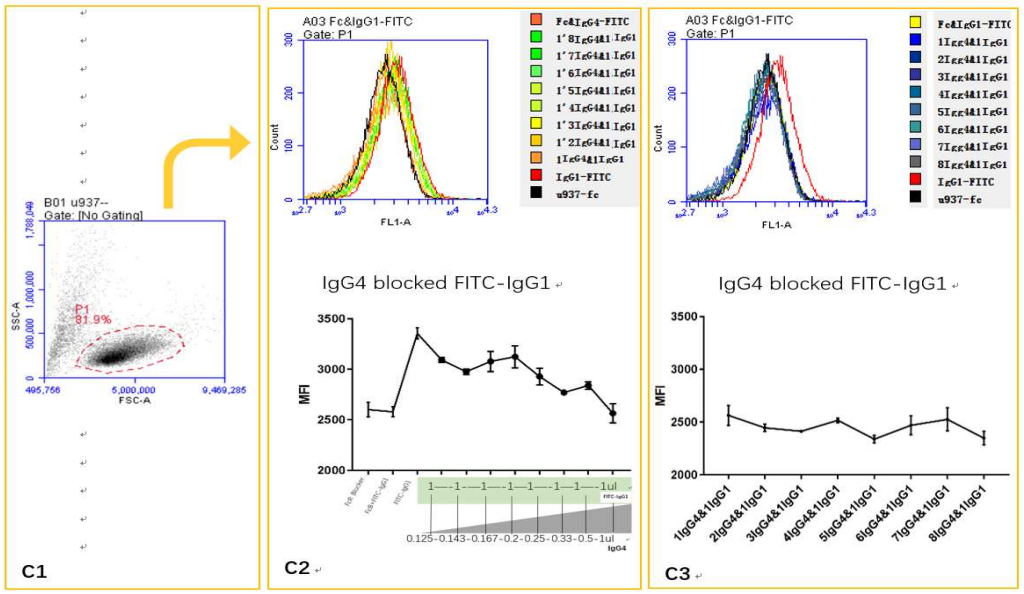

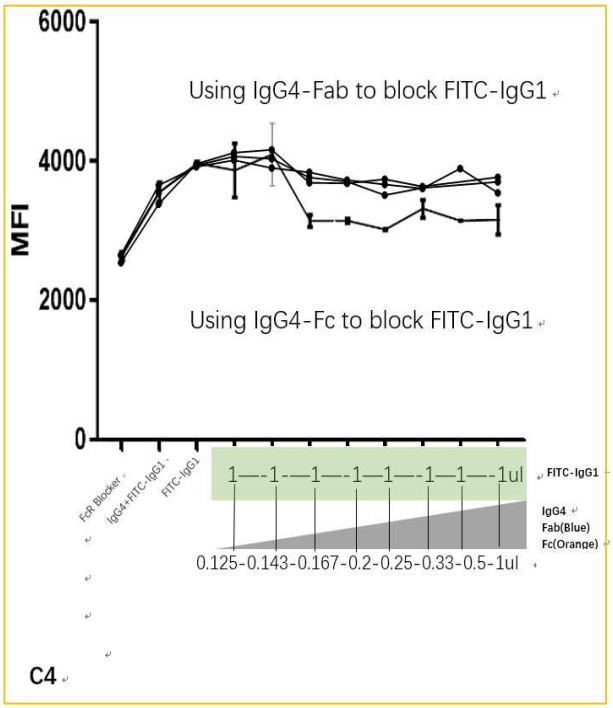

C: IgG4 blocked IgG1 in monocyte cell line U937 through fragment Fc

In order to prove whether IgG subtype has a blocking effect, we did the following experiment: IgG4 incubated with U937 cells at 4℃ for 15mins first, then added FITC-labeled IgG1 for another 15mins, washed away the excessive fluorescent protein. We then used BD C6 flow cytometer to measure cell fluorescence intensity. Unblocked U937 was used as the positive group. In order to observe the blocking effect of IgG4 on IgG1, we did 16 consecutive concentration gradients and divided charts into two parts (C2&C3) for clarity and for subsequent discussion.

***C1:** We used 10,000 cells to set the Gate P1. Living cells accounted for 81.9% of all particles. **C2:** With increasing concentrations of IgG4 (Unlabeled IgG4/FITC-IgG1 = 0.125/1;0.143/1; 0.167/1; 0.2/1; 0.25/1;0.33/1; 0.5/1; 1/1) IgG1 binding was blocked by IgG4. (n=3, P<0.01). **C3:** Showing continuous increase of the concentrations of IgG4 (1/1; 2/1; 3/1; 4/1; 5/1; 6/1; 7/1; 8/1), MFI did not change significantly. **C4**: We digested unlabeled IgG4 into two fragments Fab and Fc, and*

then to block FITC-IgG1 respectively. We found that It was the Fc fragment of IgG4 blocked the binding (three upper lines are Fab blocking groups, and the line below is the Fc group).

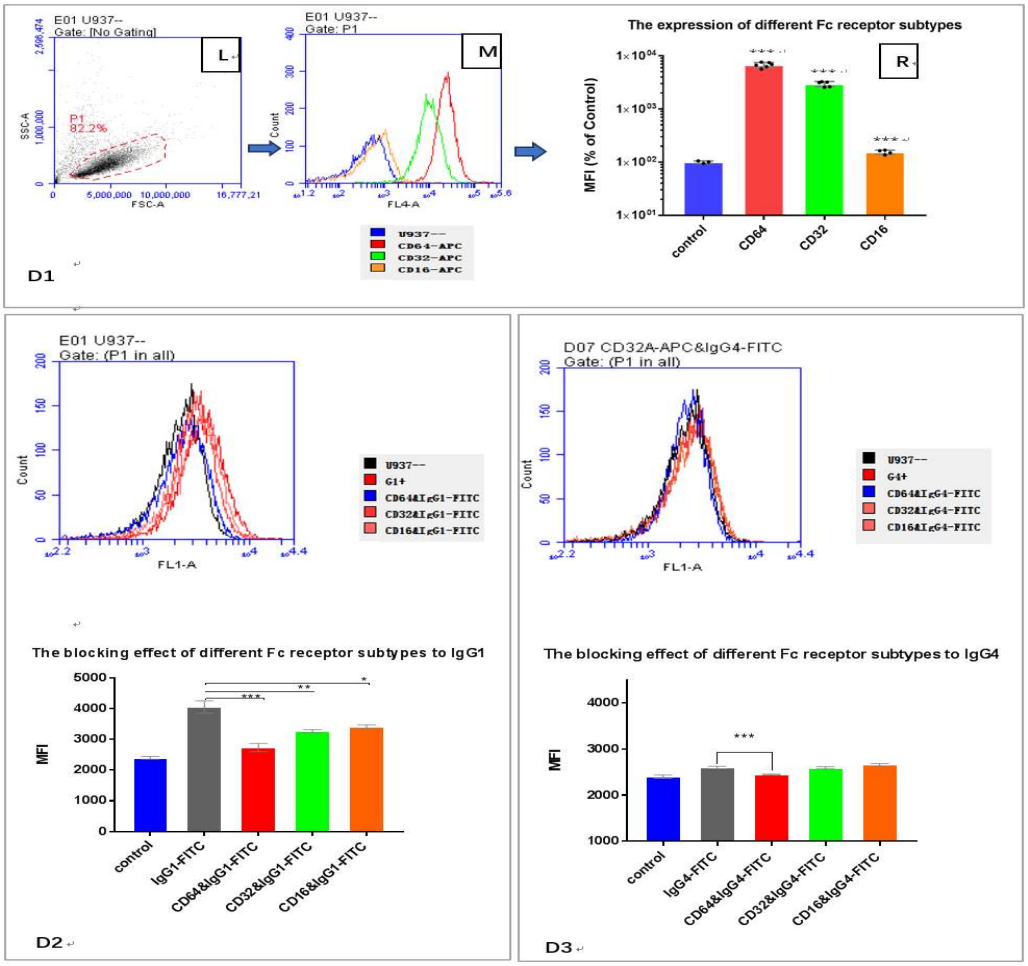

D: Different binding sites for IgG1 and IgG4 in monocyte cell line U937

In order to clarify whether IgG4's blocking effect was through the Fc receptors, we designed the following experiment. Figure D & Figure E. ***D1:*** *Confirmed the expression of Fc receptor and its subtypes on cell surface.* ***D2 & D3:*** *Blocked those three FcγRs with specific antibodies respectively, confirming that IgG1 & IgG4 have different binding sites.*

D1: *Three kinds of FcγR: FcγRI (CD64), FcγRII (CD32), FcγRIII (CD16) expressions in the mononuclear cell line U937, used APC labeled mouse anti human antibody, the left shows Gate situation, FSC represents cell diameter, and SSC represents cell internal complexity. The same cells form the charts on the right. In the middle chart, the horizontal coordinate is fluorescence intensity (FI), and the higher the FI is the higher the expression of the FcγR-X on the cell membrane, and the vertical coordinate represents the number of cells in the corresponding FI. The left image shows the MFI of the three receptors on the surface of U937 cells which is a summary of the middle chart. The negative group was calculated as 100%. The expressions of the three*

FcγR receptors of U937 can be seen in this diagram, showing the expressions of FcγRI (CD64)> FcγRII (CD32)>>FcγRIII (CD16) (n=5, p<0.001). ***D2:*** *The binding of IgG1 and U937 was blocked by all three antibodies, FcγRI (CD64) played a major role. FcγRI (CD64)> FcγRII (CD32)>>FcγRIII (CD16) (n=3, p<0.001)* ***D3:*** *The binding of IgG4 and U937 was blocked by FcRγI (CD64) antibody only (n=3, p<0.001).*

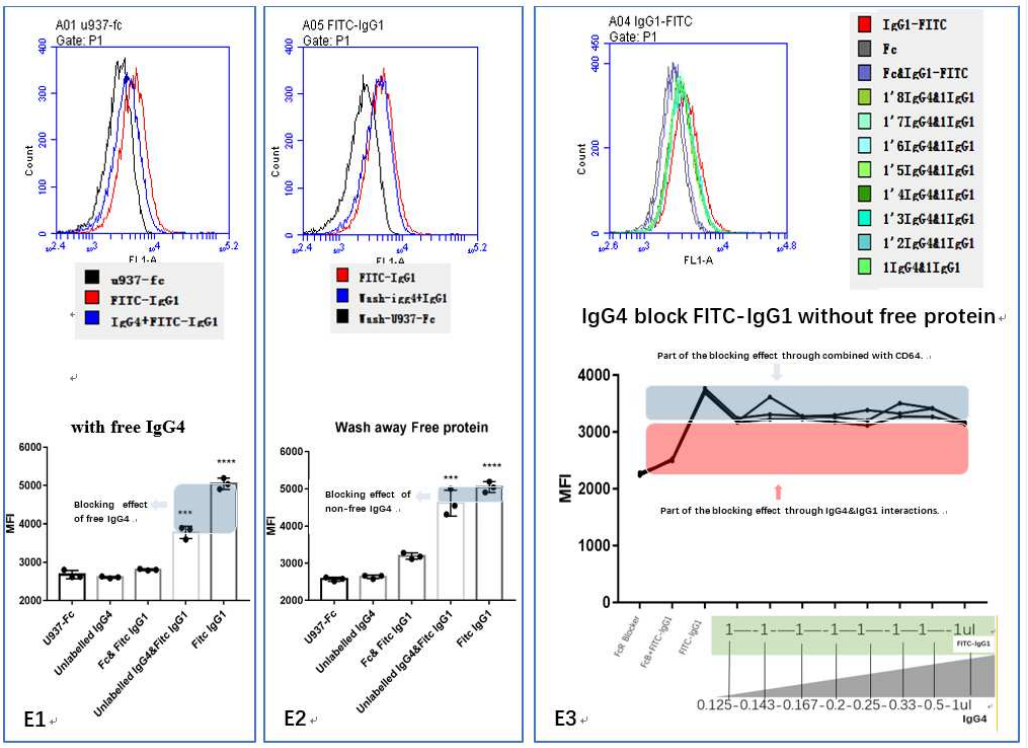

E: Continued presence of IgG4 in solution is necessary for competition with IgG1 for FcγR

As shown above, IgG4 has a low binding force with Fc receptor and is different in its binding site from that of IgG1, but it completely blocked IgG1 at the same concentration (1:1). Therefore, we hypothesize that IgG4 in the solution, rather than at the site of the receptor, might play a role in the IgG1 blocking experiment. So we did two more experiments. IgG4 was incubated with U937 cells at 4°C for 15mins first, and then the cells were divided into two groups. In one group ***(E1),*** *FITC-labeled IgG1 was added to incubate with U937 cells at 4°C for 15mins, and the excessive fluorescent protein solution was washed away, then the BD C6 flow cytometer was used to measure cell fluorescence intensity. In another group* ***(E2)****, after 15mins incubation, we washed away the unbound IgG4, and then added FITC-labeled IgG1 to incubate with U937 cells at 4°C for 15mins directly. After washing away the excess fluorescent protein, we used BD C6 flow cytometer to measure cell fluorescence intensity.*

E1 & E2: *When the FITC-IgG1 and U937 were incubated, the blocking effect of IgG4 was better when there was free IgG4 in the solution than when the IgG4 was removed from the solution.* ***E3:*** *When IgG4 was removed from the reaction solution, increasing the concentration of IgG4 (unlabeled*

IgG4/FITC-IgG1 = 0.125/1;0.143/1; 0.167/1; 0.2/1; 0.25/1;0.33/1; 0.5/1; 1/1) did not increase the binding of IgG4 to monocytes. Therefore, the blocking effect was not changed. Comparing with ***C3****, where IgG4 completely blocked IgG1 under the same concentration gradient (1:1). The concentration gradient of IgG4 in the solution appeared to be necessary for it to compete with IgG1 to bind to the receptors.* ***E3:*** *This is an extension of* ***E2,*** *where eight continuous concentration gradients were tested to further verify the trend. Although IgG4 and IgG1 have their respective preferred receptor subtypes, IgG4 could completely block the binding of IgG1 to its preferred receptors on the surface of monocytes. We speculate that the 3-D structure of IgG4 might interfered or shielded the interaction between IgG1 and its receptors. In addition, these experiments showed that continued presence of certain concentration of IgG4 in the solution is necessary for it to effectively block IgG1 binding to its receptors. This might explain the inhibitory effect of IgG4 in human cancer microenvironment where IgG4 was significantly increased and this will facilitate IgG4 to bind to Fc receptors in place of IgG1, thereby reducing local immune reaction.*

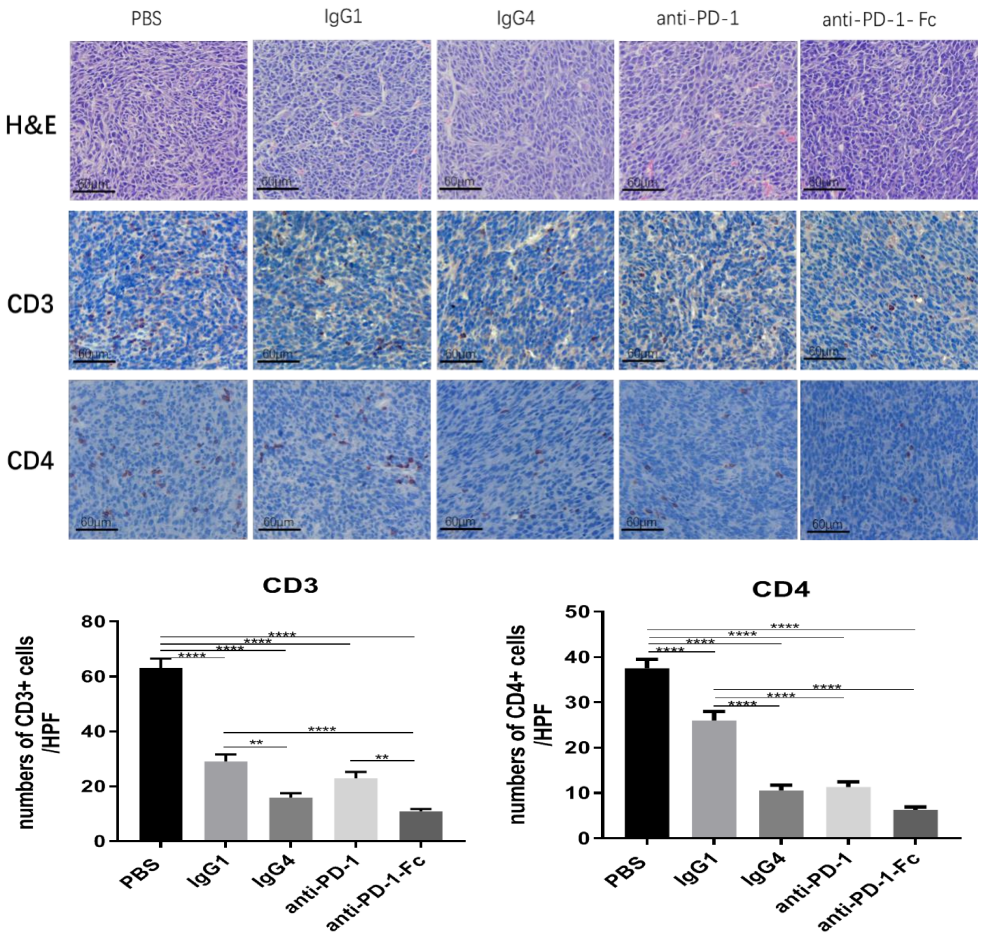

Figure S9, T lymphocytes were significantly decreased in colon cancer treated with IgG4.

Upper photos show tumor morphology of the colon cancer (CT26) animal model. The first panel shows H&E staining of the tumor treated with different reagents as labeled on the top. The second and third panels show representative immunohistochemistry images and quantification of total T lymphocytes (CD3+) and helper T-cells (CD4+) respectively in the tumor microenvironment. The positive T lymphocytes are shown as small brown spots. Original magnification ×20. The bar charts below indicate the numbers of positive cells in different treatment groups (IgG1/IgG4/ Nivolumab and its Fc fragment as well as the control (PBS) (n=5 mice/group). IHC analysis for CD3+ and CD4+ T cells showed that T cells were significantly decreased in treated groups (with non-cancer-specific IgG4 including Nivolumab, and to a lesser extent with non-cancer-specific IgG1).

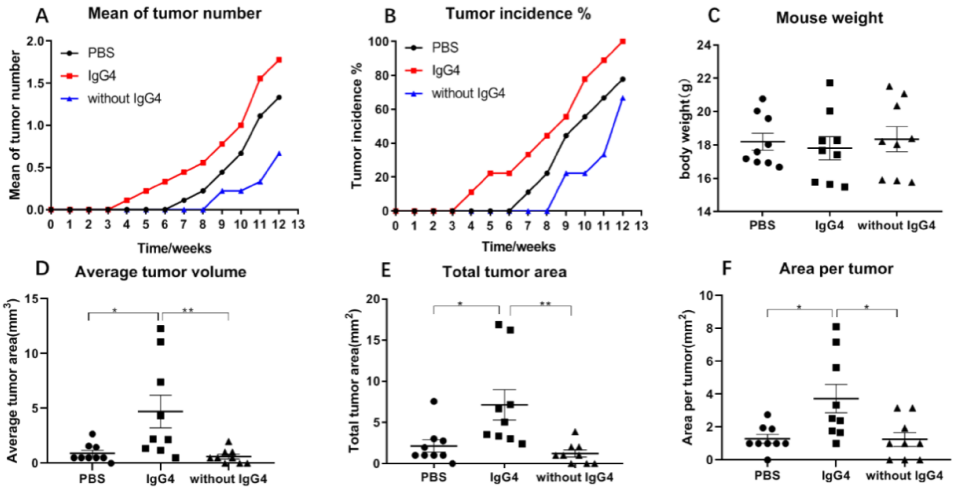

Figure S10. Application of IgG4 significantly promoted DMBA/TPA-induced skin tumor.

A: *The dynamic growth curve of mean numbers of papillomas in each treated groups.* ***B:*** *The incidence of papillomas in each treated groups.* ***C:*** *Mouse weight on day 85 (3 groups had no difference).* ***D:*** *Tumor volume of tumor-bearing mice in each group.* ***E & F:*** *Total tumor number and tumor area of each mouse in each group. The results clearly showed that IgG4 promoted skin tumor progression in both number and size.*

Methods

Immunohistochemistry

Tissue samples were fixed in 4% paraformaldehyde and then embedded in paraffin. Serial sections were cut at 3.5μm, thickness on a microtome (Leica) and dried at 60℃ for 4-6 hours. Before staining, sections were deparaffinized with 10-minute incubation with xylene 3 times and then rehydrated through a graded alcohol series. Heat-induced antigen retrieval was performed in a 95℃ water bath for 15 minutes in a microwave oven, using Tris-EDTA pH9 retrieval buffer. The samples were incubated with 3% hydrogen peroxide for 20 minutes to block endogenous peroxidases, and horse serum was used to block non-specific binding. Subsequently,

sections were stained with a standard immunohistochemistry procedure with the following commercial antibodies: Mouse anti-human IgG1 (ZSGB-BIO), rabbit anti-human IgG2 (Abcam), rabbit anti-human IgG3 (Abcam) and rabbit anti-human IgG4 (Abcam). Primary antibodies were detected with goat anti-mouse/anti-rabbit IgG (PV-9000, ZSGB-BIO), and immunoreactivity was developed with an AEC kit (GBI). The sections were counterstained with hematoxylin. All sections were mounted with glycerin jelly mounting solution (Beyotime) and finally the slides were scanned with a digital microscope scanning system (EasyScan, Motic BA600, Xiamen, China) using ×10, ×20 and ×40 magnification lenses.

Measurement of IgG4 concentrations in tumor and adjacent normal tissues with Enzyme-linked ImmunoSorbent Assay (ELISA)

ELISA assay to measure IgG4 concentrations in tumor and tumor-adjacent normal tissue was performed based on a protocol described previously(1, 2). Frozen tissues were sheared and homogenized for ELISA analysis. Tissue were weighed and recorded. RIPA lysate buffer (CA#92590, Millipore, USA), together with protease inhibitor (CA#78425, Thermo Fisher, USA) was added in tissue and lysated on ice for 30 minutes. After lysis, centrifugation was carried out at 10000 rpm/min for 15 minutes to collect the supernatant. The supernatant was measured for IgG4 with an IgG4 ELISA kit (CA#EHC147.96, Neobioscience Technology, Shenzhen, China). The supernatant was diluted 10 times with sample diluent. Sample diluent (100μL) was added to blank wells in duplicate and incubated for 2 hours at 37℃, After washing 5

times with 200μL washing solution, 100μL of diluted enzyme-conjugated antibody to all wells and incubated for 1 hours at 37℃. After washing 5 times with washing buffer, 100μL of TMB substrate solution was pipetted to all wells and incubated for 15 minutes. Stop solution was added when the wells had developed into a dark blue color. The enzyme reaction was stopped by quickly pipetting 100μL of stop solution into each well. The reaction density of each microwell was read on a spectrophotometer at 450 nm.

IgG4 immunohistochemistry

We first applied the primary antibodies (IgG1, not labeled) to corresponding tissue sections and incubated at 4℃ overnight. After washing with buffer, biotin-labeled IgG4 (not antigen-specific, or IgG1-specific) was applied to the tissue section and incubated for another hour at room temperature. After washing, the labeling biotin was visualized with a 3-amino-9-ethylcarbazole (AEC) detecting kit. The locations of the corresponding antigens were demonstrated.

Measurement of distances between different subtypes of B lymphocytes in cancer

On each esophageal cancer slide, two subtypes of B lymphocytes were double-immunostained resulting in red and green fluorescent colors for two different subtypes of B cells. The distances between two different subtypes of B cells (between IgG4 and IgG1 positive cells, between IgG4 and IgG2 positive cells, and between IgG4 and IgG3 positive cells) were measured in ten (10) cases of esophageal cancers

(five 40X randomly selected fields in each cancer) with an Image Pro Plus software (Maryland, USA). The pixel data were converted into the length in μm and treated statistically with GraphPad Prism 7.0 (San Diego, USA). The differences between different pairs of B cell types were compared.

Protein Preparations

IgG labeling: IgG1 and IgG4 were purchased from Athen Research USA (IgG1, human Myeloma Plasma, Kappa, #16-16-090707-1M; IgG4, human Myeloma Plasma, Kappa, #16-16-090707-4M). FITC Antibody Labeling Kit was purchased from Thermo Scientific™ USA (FITC Protein Labeling Kit, # F6434). Protein labeling was carried according to the instruction. Briefly, add 40 μL Borate Buffer (0.67M) to 0.2mL of 2mg/mL protein in PBS to make a pH 8.5 labeling buffer, add FITC Reagent, calculate the volume of the FITC Reagent to be added using the following formula: μL FITC Reagent =mg/mL protein × 0.2 mL× 389 × 100 × MR/MW protein. Mixt at room temperature for approximately 1 hour, add the reaction fluid to the purification resin to remove the unbound FITC. Measure the absorbance with enzyme standard instrument Epoch2 at 280 nm (A280) and 494 nm (A494) to determine the degree of labeling.

Papain digestion

Use Zeba Spin Desalting Column to replace protein solution to 3.5mg/mL Cysteine-HCl Digestion Buffer, wash Papain bound resin with Fab Digestion Buffer,

add the desalted IgG to the resin, incubate the digestion reaction 5-6 hours at 37°C in mixer. Centrifuge column at 5000 × g for 1 minute to separate digest from the immobilized Papain, save the flow-through. Preparing a NAb Protein A Plus Spin Column, load the flow-through to Protein A column, mix for 10 minutes, centrifuge for 1 minute, collect the flow-through as this fraction contains Fab fragments. Wash column with PBS, add IgG Elution Buffer to Protein A Column and centrifuge for 1 minute collect the flow-through as this fraction contains Fc fragments and undigested IgG. Add 40μL of 1MTris-base to adjust pH. The Papain cutting efficiency was determined by SDS-PAGE and Silver stain.

FACS for Fc receptor assays

FITC labeled IgG incubates with U937 cells in 4℃ for 15mins, wash away excess fluorescent protein, use BD C6 flow cytometer to measure cell fluorescence intensity. Negative controls were cells that were not treated with fluorescent protein or treated with unlabeled IgG. In the receptor blocked experiment, FcγR Blocker (BioLegend，#422302), FcγRI Antibody (Sino-Biological,#10256-R401-A), FcγRII Antibody (Sino-Biological, #10374-MM02), FcγRIII Antibody (Sino-Biological, #10389-MM23-A) was incubated with U937 at 4°C for 15 mins respectively, then use FITC labeled IgG to incubate with FcR blocked U937 at 4 °C for 15mins, wash away excess fluorescent protein, use BD C6 flow cytometer to measure cell fluorescence intensity. In the IgG4 blocking IgG1 experiment, unlabeled IgG4 or its Fab or Fc fragment to incubate with U937 cells at 4°C for 15mins first, then add FITC labeled

IgG1 to incubate with U937 cells at 4°C for 15mins again, wash away excess fluorescent protein, use BD C6 flow cytometer to measure cell fluorescence intensity. The mean fluorescence intensity（MFI) of 1×10^4 cells was used as an index to evaluate the blocking effect.

Antibody-dependent cell-mediated cytotoxicity (ADCC) test was performed based on previously reported protocols (3-5). Peripheral blood mononuclear cells (PBMC) were separated from peripheral blood obtained from healthy donors by centrifugation with Ficoll-Paque. After the target cells (4000/well) were adheres to the well, the medium was removed. Target cells and PBMC from healthy donors as effector cells were co-incubated at 40:1 effector/target ratios in 100μL of RPMI 1640 containing 10% FBS(v/v), 100U/mL penicillin and 100μg/mL streptomycin in a 96-well culture plates in quadruplicate with i.e, Cetuximab (3μg/mL), IgG4, IgG1, and human serum albumin (HSA) as group 1, Cetuximab plus IgG4 as group 2, Cetuximab plus IgG1 as group 3 and Cetuximab plus HSA as group 4. After incubation for 24hr at 37°C, 10μLof CCK8 was added to each well and incubation was carried out for another 1-3 hr. Cell-free 1640 medium was added as a blank group. The absorbance was measured at 450nm with a microplate reader.

In the Fc receptor blocking experiment，Tumor cells were plated in 96-well plates, treated with Ab or protein. Then cultured with PBMC (from peripheral blood of healthy volunteers) which had been treated with Fc receptor blocker Human TruStain

FcX™（BioLegend, USA). Cell proliferation was evaluated with a CCK8 kit (Dojindo, Japan).

Antibody-dependent cellular phagocytosis (ADCP) assays were performed following previously reported protocols (4, 6-8). Lung cancer cell line A549 (expressing EGFR) was used as the targets, human peripheral monocyte-derived macrophages as the effector cells and the antibody Cetuximab (IgG1) against EGFR as the mediating antibody. Briefly, the tumor cells (A549) were stained with CFSE-DA fluorescence probes (C0051, Beyotime) and macrophages derived from PBMC were stained with DiI fluorescent probes (C1036, Beyotime). Cells were co-cultured in 24-well plate (Macrophage/A549 =10/1) and Cetuximab was added to the co-culture system as the positive control in the experimental group. Different concentrations of IgG4 and Cetuximab were simultaneously added to the co-culture system. None Cetuximab group was used as the negative control. Results were analyzed with a fluorescence microscopy (Life evos) and flow cytometry (BD Accuri C6). Under the fluorescence microscope we can see that a part of the macrophages recognize and devour the tumor cells, we count the percentage of these macrophages as an indicator of phagocytosis. The counting was performed on 30 randomly selected field at 20× magnification for each group. In flow cytometry, CFSE-DA labeled A549 were positive in FL1, while macrophages were negative. We calculated the number of tumor cells after 24 hours of co-culturing to evaluate the effect of tumor cell killing.

Complement-dependent cytotoxicity (CDC) assays were performed based on the previously reported procedures (9-11). For CDC assays, target A549 cells were digested with 0.25% trypsin and washed with medium by centrifugation and resuspension. The cells were then seeded at 25,000 cells per well in 96-well plates in triplicate. After the cells are attached, add the antibody (cetuximab, 4μg/mL) and protein (IgG1 or IgG4, 20μg/mL) was added and incubated for 30 minutes. Human plasma, which was obtained from healthy volunteers and served as a source of complement. Final complement concentration was 25% (diluted with PBS buffer). Inactivated serum (56℃, 30min） was used as a negative control. Plates were incubated for 2 h at 37℃. Target cell viability was measured with addition of 10μL Cell Counting Kit-8 for 1-2 h at 37℃. The absorbance was measured at 450nm with the microplate reader.

IgG4 was obtained from human myeloma plasma (Athens Research & Technology, Inc). In a different group, IgG4 was excluded from total IgG (IVIG) (Shanghai, China) with a column coated with specific antibody to IgG4. The flow-through IgG is “IgG without IgG4”. The possible presence of IgG4 in the preparation was verified with Western blot and biotin-labeled antibody to IgG4. No positive band of IgG4 was observed in the preparation.

Mouse breast cancer (4T1) model

The mice were divided into three groups, i.e. IgG4 only, IgG without IgG4 and

control (PBS). IgG4 and IgG without IgG4 were injected at 200μg/mouse (1mg/mL, 200μL). The day after the initial IgG4 injection, each mouse was inoculated with $1x10^5$ 4T1 mouse breast cancer cells ~~(ATCC, USA)~~ at the exact location of IgG4 injection. Four injections of the treatment solution were given and 5 days apart. The sizes of the tumor mass were measured and photographed every three days. The mice~~ouse~~ were sacrificed at day 21. The tumors were surgically removed and weighted.

Mouse colon cancer (CT26) model

BALB/c mice were used in all experiments. All mice were purchased from Vital River technical co. LTD (Beijing, China) and maintained in Shantou University Medical College laboratory animal center. All experiments were conducted based on the protocols approved by the Animal Care and Use Committee of Shantou University Medical College according to the guidelines for Laboratory Animal Sciences.

All mice were aged between 6 to 8 weeks and weighted 20±2g. Twenty-five mice were randomly grouped (n=5 mice/group) and injected subcutaneously (s.c) in the right front flank with 100ug anti-PD-1, IgG4, IgG1, anti-PD-1-Fc, or control (PBS). One day after the first injection,$1x10^5$ CT26 cells were inoculated at the location of the first injection, and received an additional subcutaneously treatments with 100μg anti-PD-1,IgG4, IgG1, anti-PD-1-Fc，or control PBS on Day 5,10,15 and 19. Tumor volumes were measured every 5 days with a caliper and reported as volume using the formula $(A^2×B)/2$, where A is the shortest diameter and B is the longest diameter. All

mice were sacrificed at days 20. Tumors were harvested from sacrificed mice and weighted. All values are listed as mean±SEM for each group. (*p<0.05, **p<0.001, two-way ANOVA)

Carcinogen-induced skin tumor model

6-week-old BALB/c female mice were purchased from Vital River technical co., LTD (Beijing, China). 7,12-dimethylbenz (a) anthracene (DMBA) (D3245), 12-O-tetradacanoylphorbol-13-acetate (TPA) (P1585) were both obtained from Sigma Chemical Co. (USA), and IgG4 (16-16-090707-4M) was obtained from Athens Research and Technology. In a different group, IgG4 was immunologically removed from total IgG (IVIG) (Chengdu, China) with a column coated with specific antibody to IgG4 (Cat. No. 290005, Thermo Scientific). The flow-through IgG is "IVIG without IgG4". The possible presence of IgG4 in the preparation was verified with Western blot and biotin-labeled antibody to IgG4. No positive band of IgG4 was observed in the preparation. Skin chemical carcinogenesis was performed as follows. Two-stage skin carcinogenesis was conducted as described previously (12, 13). After 1 week of adaptation a region of posterior dorsal skin (about 2cm × 2cm) of all experimental mice were shaved for the experiments. 24 hour later, DMBA (100μg/200μL of acetone) was applied topically on the shaved area two times a week for 2 weeks, followed by TPA (5μg/100μL of acetone) 2 times a week for 13 weeks. After 2 weeks of DMBA, the mice were randomly divided into three groups (n = 9) i.e. IgG4 only, IVIG without IgG4 (hereinafter referred to as without IgG4) and

control (PBS) respectively. IgG4 and without IgG4 were injected at 200μg/mouse (1mg/mL, 200μL) subcutaneously at the same region that received TPA after each application. The papillomas, which existed for two weeks or longer, were taken into account for the final assessment of tumor development. The incidence of skin papillomas, average number of papillomas per mouse, tumour volume and area, and bodyweight were recorded at weekly intervals. Tumor analyses were calculated by using the following formulae:

Mean of tumor number = total number of papilloma in each group/number of living mice in the group.

Tumor incidence % = number of tumor-bearing animals in each group/number of mice in the group×100%

Total tumor area (mm^2) =∑tumor area/mouse

Area per tumor (mm^2) = Total tumor area/numbers of tumors/mouse

Total tumor volume (mm^3) = $1/2ab^2$ (a is the longest diameter of the tumor, and b is the length perpendicular to the longest diameter)

Average tumor volume (mm^3) = Total tumor volume/numbers of tumors/mouse

Mean tumor burden = mean tumor volume × mean number of tumors

References

1. Szubert S, Szpurek D, Moszynski R, Nowicki M, Frankowski A, Sajdak S, et al. Extracellular matrix metalloproteinase inducer (EMMPRIN) expression correlates positively with active angiogenesis and negatively with basic fibroblast growth factor expression in epithelial ovarian cancer. J Cancer Res Clin Oncol. 2014;140(3):361-9.

2. Lee SY, Bae CS, Choi YH, Seo NS, Na CS, Yoo JC, et al. Opuntia humifusa modulates

morphological changes characteristic of asthma via IL-4 and IL-13 in an asthma murine model. Food & nutrition research. 2017;61(1):1393307.

3. Shinkawa T, Nakamura K, Yamane N, Shoji-Hosaka E, Kanda Y, Sakurada M, et al. The absence of fucose but not the presence of galactose or bisecting N-acetylglucosamine of human IgG1 complex-type oligosaccharides shows the critical role of enhancing antibody-dependent cellular cytotoxicity. The Journal of biological chemistry. 2003;278(5):3466-73.

4. Watanabe M, Wallace PK, Keler T, Deo YM, Akewanlop C, Hayes DF. Antibody dependent cellular phagocytosis (ADCP) and antibody dependent cellular cytotoxicity (ADCC) of breast cancer cells mediated by bispecific antibody, MDX-210. Breast cancer research and treatment. 1999;53(3):199-207.

5. Keler T, Graziano RF, Mandal A, Wallace PK, Fisher J, Guyre PM, et al. Bispecific antibody-dependent cellular cytotoxicity of HER2/neu-overexpressing tumor cells by Fc gamma receptor type I-expressing effector cells. Cancer research. 1997;57(18):4008-14.

6. Overdijk MB, Verploegen S, Bogels M, van Egmond M, Lammerts van Bueren JJ, Mutis T, et al. Antibody-mediated phagocytosis contributes to the anti-tumor activity of the therapeutic antibody daratumumab in lymphoma and multiple myeloma. mAbs. 2015;7(2):311-21.

7. Golay J, Da Roit F, Bologna L, Ferrara C, Leusen JH, Rambaldi A, et al. Glycoengineered CD20 antibody obinutuzumab activates neutrophils and mediates phagocytosis through CD16B more efficiently than rituximab. Blood. 2013;122(20):3482-91.

8. Richards JO, Karki S, Lazar GA, Chen H, Dang W, Desjarlais JR. Optimization of antibody binding to FcgammaRIIa enhances macrophage phagocytosis of tumor cells. Molecular cancer therapeutics. 2008;7(8):2517-27.

9. Klausz K, Berger S, Lammerts van Bueren JJ, Derer S, Lohse S, Dechant M, et al. Complement-mediated tumor-specific cell lysis by antibody combinations targeting epidermal growth factor receptor (EGFR) and its variant III (EGFRvIII). Cancer science. 2011;102(10):1761-8.

10. Wirt T, Rosskopf S, Rosner T, Eichholz KM, Kahrs A, Lutz S, et al. An Fc Double-Engineered CD20 Antibody with Enhanced Ability to Trigger Complement-Dependent Cytotoxicity and Antibody-Dependent Cell-Mediated Cytotoxicity. Transfusion medicine and hemotherapy : offizielles Organ der Deutschen Gesellschaft fur Transfusionsmedizin und Immunhamatologie. 2017;44(5):292-300.

11. Goswami MT, Reka AK, Kurapati H, Kaza V, Chen J, Standiford TJ, et al. Regulation of complement-dependent cytotoxicity by TGF-beta-induced epithelial-mesenchymal transition. Oncogene. 2016;35(15):1888-98.

12. Abel EL, Angel JM, Kiguchi K, DiGiovanni J. Multi-stage chemical carcinogenesis in mouse skin: fundamentals and applications. Nat Protoc. 2009;4(9):1350-62.

13. Monga J, Chauhan CS, Sharma M. Human epithelial carcinoma cytotoxicity and inhibition of DMBA/TPA induced squamous cell carcinoma in Balb/c mice by Acacia catechu heartwood. J Pharm Pharmacol. 2011;63(11):1470-82.